Figure S1

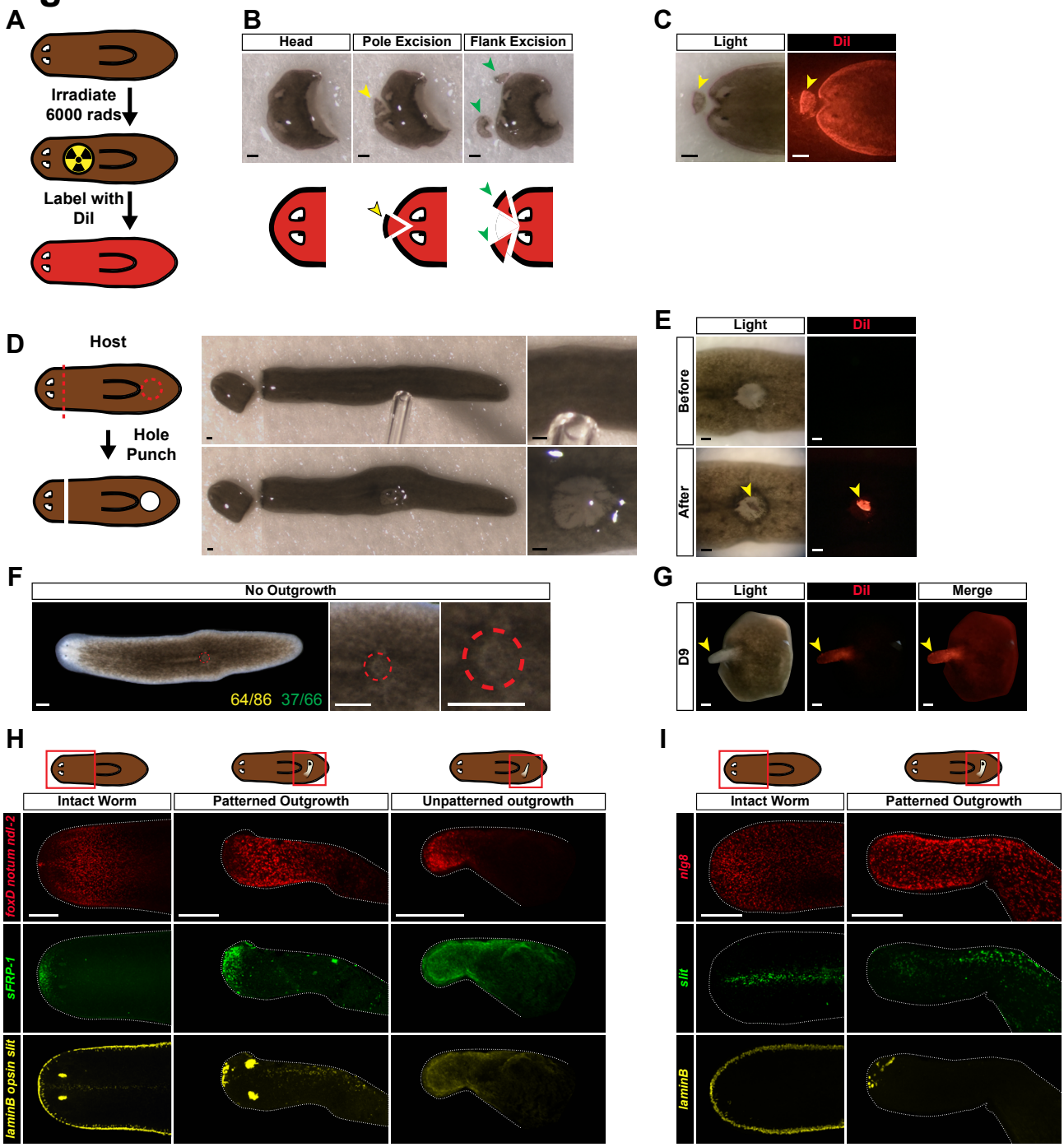
A
Irradiate
6000 rads
Label with
DiI
B
Head
Pole Excision
Flank Excision
C
Light
DiI
D
Host
Hole
Punch
E
Light
DiI
Before
After
F
No Outgrowth
64/86
37/66
G
Light
DiI
Merge
D9
H
Intact Worm
Patterned Outgrowth
Unpatterned outgrowth
foxD notum ndl-2
sFRP-1
laminB opsin slit
I
Intact Worm
Patterned Outgrowth
nlg8
slit
laminB

Figure S2

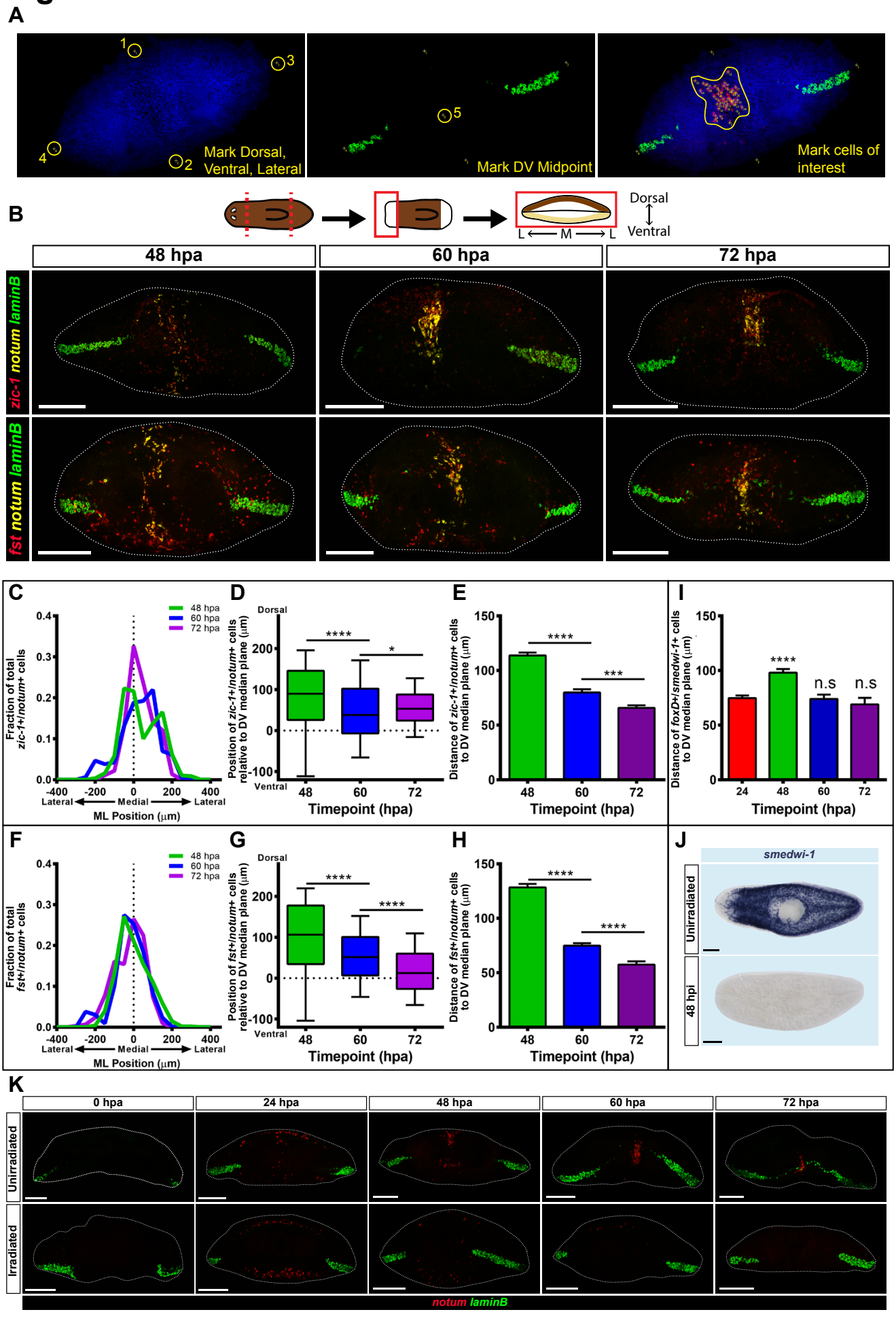
A
1
2
3
4
5
Mark Dorsal, Ventral, Lateral
Mark DV Midpoint
Mark cells of interest
B
Dorsal
Ventral
L
M
L
48 hpa
60 hpa
72 hpa
zic-1 notum laminB
fst notum laminB
C
48 hpa
60 hpa
72 hpa
Fraction of total zic-1+/notum+ cells
ML Position (μm)
Lateral
Medial
Lateral
D
Dorsal
Ventral
Position of zic-1+/notum+ cells relative to DV median plane (μm)
****
*
Timepoint (hpa)
E
Distance of zic-1+/notum+ cells to DV median plane (μm)
****
***
Timepoint (hpa)
I
Distance of foxD+/smedwi-1+ cells to DV median plane (μm)
****
n.s
n.s
Timepoint (hpa)
F
48 hpa
60 hpa
72 hpa
Fraction of total fst+/notum+ cells
ML Position (μm)
Lateral
Medial
Lateral
G
Dorsal
Ventral
Position of fst+/notum+ cells relative to DV median plane (μm)
****
****
Timepoint (hpa)
H
Distance of fst+/notum+ cells to DV median plane (μm)
****
****
Timepoint (hpa)
J
smedwi-1
Unirradiated
48 hpi
K
0 hpa
24 hpa
48 hpa
60 hpa
72 hpa
Unirradiated
Irradiated
notum laminB

Figure S3

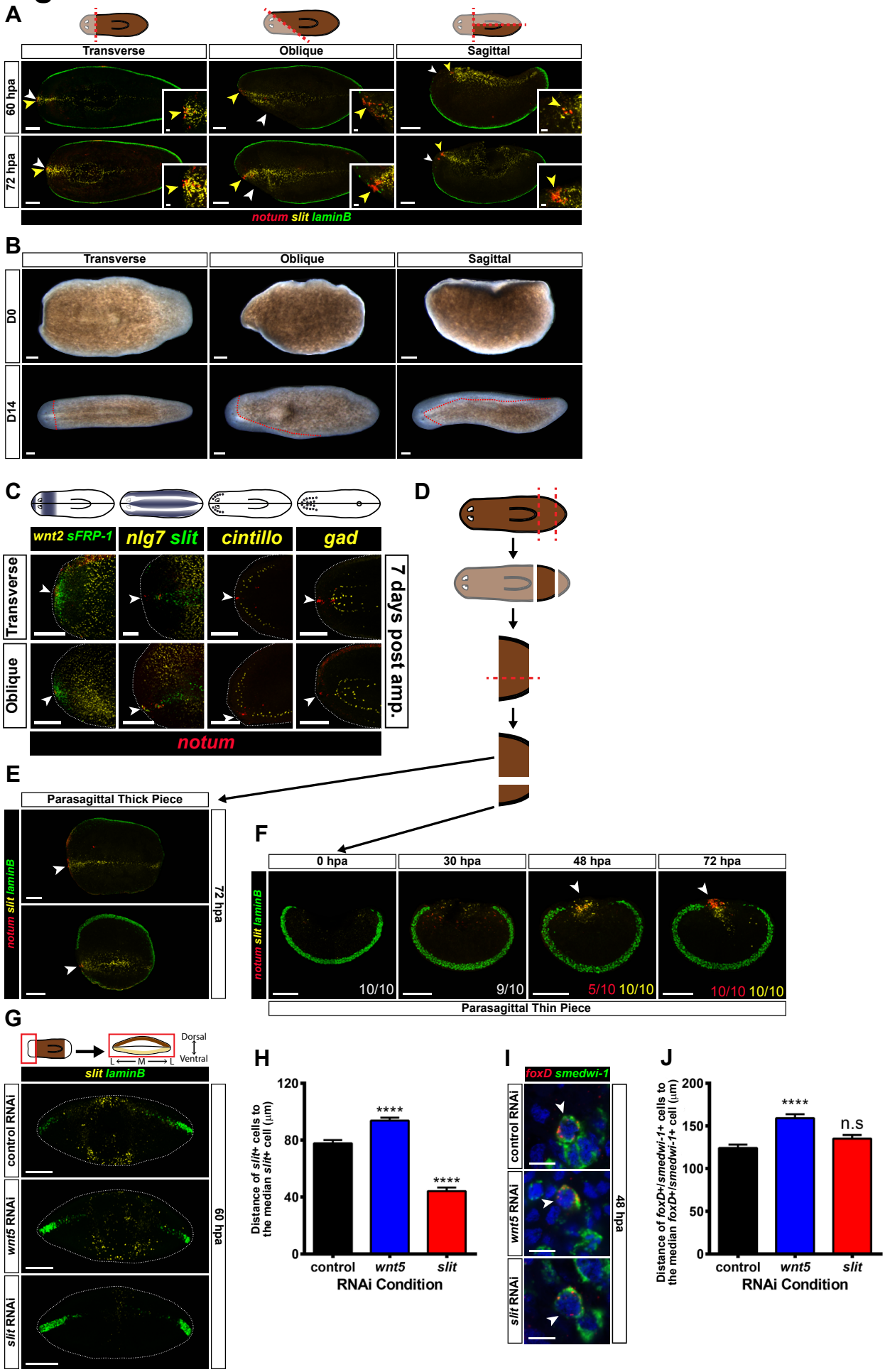
A
Transverse
Oblique
Sagittal
60 hpa
72 hpa
notum slit laminB
B
Transverse
Oblique
Sagittal
D0
D14
C
wnt2 sFRP-1
nlg7 slit
cintillo
gad
Transverse
Oblique
7 days post amp.
notum
D
E
Parasagittal Thick Piece
notum slit laminB
72 hpa
F
0 hpa
30 hpa
48 hpa
72 hpa
notum slit laminB
10/10
9/10
5/10 10/10
10/10 10/10
Parasagittal Thin Piece
G
Dorsal
Ventral
L ⟵ M ⟶ L
slit laminB
control RNAi
wnt5 RNAi
slit RNAi
60 hpa
H
Distance of slit+ cells to the median slit+ cell (µm)
120
80
40
0
****
****
control
wnt5
slit
RNAi Condition
I
foxD smedwi-1
control RNAi
wnt5 RNAi
slit RNAi
48 hpa
J
Distance of foxD+/smedwi-1+ cells to the median foxD+/smedwi-1+ cell (µm)
200
150
100
50
0
****
n.s
control
wnt5
slit
RNAi Condition

Figure S4

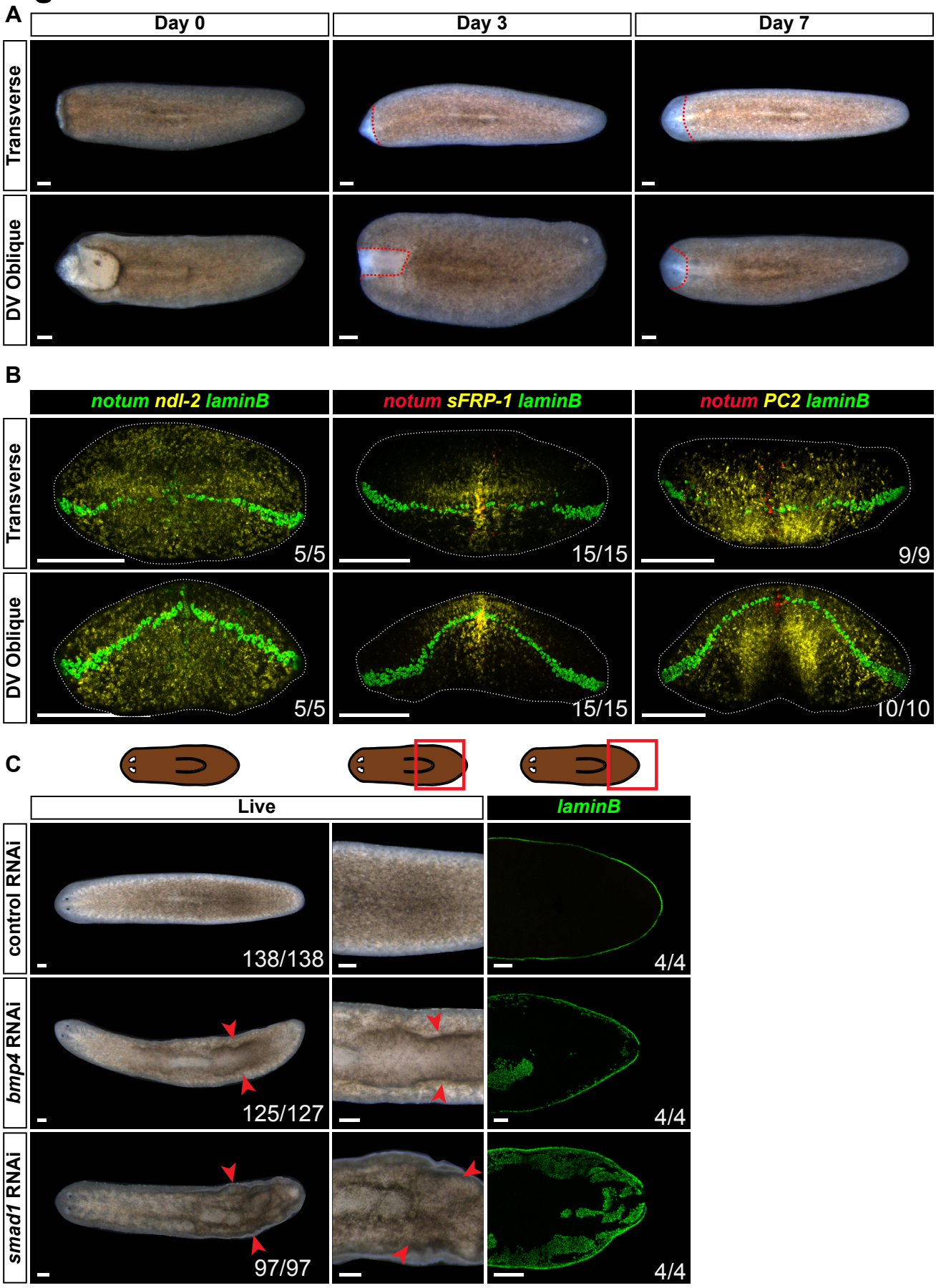
A
Day 0
Day 3
Day 7
Transverse
DV Oblique
B
notum ndl-2 laminB
notum sFRP-1 laminB
notum PC2 laminB
Transverse
DV Oblique
5/5
15/15
9/9
5/5
15/15
10/10
C
Live
laminB
control RNAi
bmp4 RNAi
smad1 RNAi
138/138
4/4
125/127
4/4
97/97
4/4

Supplemental Figure Legends

Figure S1. Pole transplantation procedure and outcomes. Related to Figure 1.

(A) Donors were lethally irradiated (6000 rads) 24 hours prior to transplantation. Animals were incubated in a 1:500 dilution of DiI (2 μg/mL) in planaria H2O overnight.

(B) The donors' heads were amputated. From a single donor, a pole piece was excised, and transplanted, and then two flank pieces were excised, and transplanted.

(C) The donor heads and pole fragments were positive for DiI signal.

(D) Hosts were placed on a filter paper over ice, and a glass capillary was used to create a "hole punch" wound in the host.

(E) The pole fragment or flank fragment was transplanted into the "hole punch" wound, and the animals was placed in a recovery chamber.

(F) A majority of transplantations resulted in no outgrowth. n=64/86 pole transplants and n=37/66 flank transplants resulted in no outgrowth. A red dotted circle marks the site of failed outgrowth.

(G) Outgrowths were positive for DiI signal, indicating that the outgrowths contained donor tissue. **(B-G)** Dorsal view, anterior is to the left. Scale bars, 200 μm.

(H) Animals were labeled using RNA FISH for the expression of *foxD/notum* (anterior pole), *sFRP-1* (anterior head tip), *slit* (midline), *ndl-2* (pre-pharyngeal region), *opsin* (photoreceptor neurons), *laminB* (DVB). Single-channel images are displayed. For merged images see Figure 1B.

(I) Animals were labeled using RNA FISH for the expression of *nlg8* (red), *slit* (green), and *laminB* (yellow). Single-channel images are displayed. Pole transplant outgrowths have entirely dorsal identity (n=4/4) **(H-I)** Images shown are maximal intensity projections. Dorsal view, anterior is to the left. Scale bars, 200 μm.

Figure S2. Anterior pole progenitors are specified medially and in a broad DV domain. Related to Figure 1 and Figure 2.

(A) During image quantification, multiple attributes of each image were marked in the following order. The locations of the dorsal-most point, ventral-most point, and the two lateral-most points were marked. The location of the estimated DV median plane was marked using *laminB* signal as a guide. The positions of the cells of interest were marked.

(B) Wild-type animals were subjected to a transverse amputation, fixed at 48, 60 and 72 hpa, and expression of either *zic-1* or *follistatin* (red), and *notum* (yellow) and *laminB* (green) was analyzed by triple FISH. *zic-1+*/*notum+* and *follistatin+*/*notum+* cells appear around 48 hpa at the ML median plane of the anterior-facing wound, and accumulate over time near the DV median plane.

(**C**) The distribution of the positions of *zic-1+*/*notum+* cells on the ML axis is centered roughly around the ML median plane of the fragment (dotted line). 48 hpa, n=16 worms; 60 hpa, n=15 worms; 72 hpa, n=14 worms.

(D) The distribution of the positions of *zic-1+*/*notum+* cells on the DV axis becomes tighter over time. Data were compared with a Mann-Whitney test. 48 vs 60 hpa, ****p<0.0001, n>473 cells; 60 vs 72 hpa, *p=0.0283, n>364 cells.

(E) The distance between *zic-1+*/*notum+* cells and the DV median plane grows smaller over time. Data were compared using a Student's t-test. 48 vs 60 hpa, ****p<0.0001, n>473 cells; 60 vs 72 hpa, ***p=0.0002, n>364 cells.

(F) The distribution of the positions of *follistatin+*/*notum+* cells on the ML axis is centered roughly around the ML median plane of the fragment (dotted line). 48 hpa, n=16 worms; 60 hpa, n=16 worms; 72 hpa, n=12 worms.

(G) The distribution of the positions of *follistatin+*/*notum+* cells on the DV axis becomes tighter and closer to the DV median plane over time. Data were compared with a Mann-Whitney test. 48 vs 60 hpa, ****p<0.0001, n>479 cells; 60 vs 72 hpa, ****p<0.0001, n>298 cells.

(H) The distance between *follistatin+*/*notum+* cells and the DV median plane grows smaller over time. Data were compared using a Student's t-test. 48 vs 60 hpa, ****p<0.0001, n>479 cells; 60 vs 72 hpa, ****p<0.0001, n>298 cells.

(I) The distance between *foxD+*/*smedwi-1+* cells and the DV median plane at 60 and 72 hpa is comparable to the distance at 24 hpa. At 48 hpa this distance is increased. Data are represented as mean ± SEM and analyzed using a Student's t-test. 48 hour, 60 hour, and 72 hour timepoints were compared to 24 hpa. 48 hpa ****p<0.0001, n>311 cells, 60 hpa n.s., n>114 cells, 72 hpa n.s., n>75 cells.

(J) Colorimetric *in situ* hybridization for the expression of the gene *smedwi-1*, which marks neoblasts. 48 hours post irradiation (hpi), animals were completely depleted of neoblasts.

(K) Wild-type animals were lethally irradiated (6000 rads) 48 hours prior to injury. Irradiated and unirradiated controls were transversely amputated, fixed at 0, 24, 48, 60 and 72 hpa, and expression of *notum* (red) and *laminB* (green) was analyzed by double FISH. At 0 hpa, anterior pole expression of *notum* has been completely eliminated by transverse amputation. At 24 hpa, wound-induced *notum* expression still occurs in animals that have been lethally irradiated. From 48 to 72 hpa, anterior pole progenitors do not appear and no anterior pole is formed in animals which have been lethally irradiated. For FISH images in **(B)** and **(K)** images are an *en face* view of the anterior blastema. Dorsal is up. Scale bars, 200 μm. For colorimetric images in **(J)**, images are a ventral view, anterior is to the left. Scale bars, 200 μm. For **(D)** and **(G)** the reference point for these coordinates is the DV median plane, which is estimated using *laminB* expression (dotted line). The box is defined by the first quartile, median, and third quartile, and the whiskers are defined by the 10th and 90th percentiles. For **(E)** and **(H)** data are represented as mean ± SEM.

Figure S3. Surgeries and *wnt5*/*slit* RNAi affect the ML axis. Related to Figure 3.

(A) Wild-type animals were subjected to either a transverse, oblique or sagittal amputation, fixed at 60 and 72 hpa, and expression of *notum* (red), *slit* (yellow) and *laminB* (green) was analyzed by triple FISH. *notum+* cells appear near the *slit* domain, even when that domain is no longer the middle of the wound face. Cartoon above shows type of injury; fully opaque region indicates the fragment selected for analysis. White arrowheads indicate the estimated ML median plane of the anterior-facing wound, and yellow arrowheads indicate the old midline, as marked by *slit* expression. Transverse 60 hpa, n=6/6; Oblique 60 hpa, n=11/11; Sagittal 60 hpa, n=10/10; Transverse 72 hpa, n=8/8; Oblique 72 hpa, n=12/12; Sagittal 72 hpa, n=20/20.

(B) Wild-type animals were subjected to either a transverse, oblique or sagittal amputation, and live imaged at 0 days or 14 days after injury. Animals are capable of successfully regenerating from these amputations.

(C) Wild-type animals were subjected to either a transverse or oblique amputation as described in (A), fixed at 7 days following wounding, and expression of *notum* (red), and the following markers were analyzed by triple FISH: *wnt2* (yellow) and *sFRP-1* (green); *nlg7* (yellow) and *slit* (green); *cintillo* (yellow); and *gad* (yellow). White arrowheads mark the position of the anterior pole. For clarity, ventral images (*nlg7/slit* and *gad*) were vertically flipped to have the same orientation as dorsal images. The plane of symmetry for gene expression was centered at the position of the anterior pole, even in animals that had an asymmetric wound.

(D) Cartoon depiction of the generation of thick and thin parasagittal pieces. A series of two transverse amputations produced a trunk piece. This fragment was separated into two pieces with a sagittal amputation to the right of the ventral nerve cords.

(E) The parasagittal thick pieces were fixed at 72 hpa, and expression of *notum* (red), *slit* (yellow) and *laminB* (green) was analyzed by triple FISH. White arrowheads indicate the position of the anterior pole. The anterior pole regenerates at the pre-existing midline. Two representative examples are shown.

(F) The parasagittal thin pieces were fixed at 0, 30, 48 and 72 hpa, and expression of *notum* (red), *slit* (yellow) and *laminB* (green) was analyzed by triple FISH. White arrowheads indicate the position of the anterior pole. Immediately after the surgery, there is very little *slit* expression (10/10 animals). By 30 hpa, *slit* and wound-induced *notum* are expressed at the wound face (9/10 animals). At 48 hpa, some of the animals had begun to form a new anterior pole (5/10 animals), and all the animals had *slit* expression (10/10 animals). At 72 hpa all of the animals had formed a new anterior pole (10/10 animals), and all animals had *slit* expression extending into the fragment (10/10 animals).

(G) control RNAi, *wnt5(RNAi)* or *slit(RNAi)* animals were transversely amputated, fixed at 60 hpa, and expression of *slit* (yellow) and *laminB* (green) was analyzed by double FISH. *slit+* cells occupy a wider area in *wnt5(RNAi)*, and a narrow area in *slit(RNAi)*, compared to control RNAi animals.

(H) The distance between *slit+* cells and the median cell is larger in *wnt5(RNAi)* animals and smaller in *slit(RNAi)* animals, as compared to control RNAi animals. Data are represented as mean ± SEM and analyzed using a Student's t-test. control vs *wnt5*(RNAi), ****p<0.0001, n>621 cells; control vs *slit*(RNAi), ****p<0.0001, n>454 cells.

(I) control RNAi, *wnt5(RNAi)* or *slit(RNAi)* animals were transversely amputated, fixed at 48 hpa,, and expression of *foxD* (red) and *smedwi-1* (green) was analyzed by double FISH. Nuclear signal (DAPI) is shown in blue. *foxD+*/*smedwi-1+* cells could be found and quantified.

(J) The distance between *foxD/smedwi-1+* cells and the median cell is larger in *wnt5(RNAi)* animals as compared to control RNAi animals. Data are represented as mean ± SEM and analyzed using a Student's t-test. control vs *wnt5*(RNAi), ****p<0.0001, n>510 cells; control vs *slit*(RNAi), n.s., n>496 cells. For **(A-C) and (E-F)** images shown are maximal intensity projections. Dorsal view, anterior is to the left. Scale bars, 200 μm. Insets (where present) are a zoomed in view of the anterior-facing wound. Scale bars, 20 μm. For **(G)** images shown are maximal intensity projections. Images are an *en face* view of the anterior blastema. Dorsal is up. Scale bars, 200 μm. For **(I)** images are a single confocal slice. Images are an *en face* view of the anterior blastema. Dorsal is up. Scale bars, 10 μm.

Figure S4. DV oblique cuts and Bmp pathway inhibition affect the DV axis. Related to Figure 4.

(A) Live images of wild-type animals were subjected to either a transverse or DV oblique cut, and imaged at D0, D3 and D7 following wounding. Animals are capable of restoring form after these injuries. A red dotted line marks the old tissue/blastema boundary. Images are a dorsal view of the entire animal. Anterior is to the left. Scale bars, 200 μm.

(B) Wild-type animals were subjected to either a transverse or DV oblique amputation, fixed at 7 days following wounding and gene expression was analyzed by triple FISH. Left column: *notum* (green), *ndl-2* (yellow) and *laminB* (green). Middle column *notum* (red), *sFRP-1* (yellow) and *laminB* (green) Right column: *notum* (red), *PC2* (yellow) and *laminB* (green). Gene expression domains and tissue architecture appear to maintain their spatial relationship with the anterior pole. Number of animals that appear like the representative image are displayed in the lower right corner of each image. Images shown are maximal intensity projections. Images are an *en face* view of the anterior blastema. Dorsal is up. Scale bars, 200 μm.

(C) Left column: Live images of control RNAi, *bmp4(RNAi)* and *smad1(RNAi)* animals 28 days after the first RNAi feeding. *bmp4(RNAi)* and *smad1(RNAi)* animals display ridges on their dorsal side. Red arrowheads indicate dorsal ridges. Anterior is to the left. Scale bars, 200 μm. Middle column: Higher magnification of the posterior of the animals. Red arrowheads indicate dorsal ridges Anterior is to the left. Scale bars, 200 μm. Right column: Expression of *laminB* (green) was analyzed by single FISH. Patches of ectopic *laminB* expression can be found on the dorsal sides of *bmp4(RNAi)* and *smad1(RNAi)* animals. Number of animals with the phenotype is displayed in the lower

right corner of each image. Images shown are maximal intensity projections. Images are a dorsal view of the tail. Anterior is to the left. Scale bars, 200 μm.

Table S1. List of genes used in this study. Related to Figures 1-4.				
Gene Symbol	**Reference**	**Pubmed ID**	**NCBI Accession Number**	**Ref. No.**
bmp4	Molina 2007	17905225	EF633689	[S1]
cintillo	Oviedo 2003	12557210	AY067542	[S2]
follistatin	Roberts-Galbraith 2013	23297191	KC161222	[S3]
foxD	Vogg 2014	24704339	KC577557	[S4]
gad	Nishimura 2008	18440152	AB332029	[S5]
laminB	Tazaki 2002	12203092	AY067086	[S6]
mag-1	Zayas 2010	20865784	HM803280	[S7]
madt	Wenemoser 2010	20599901	EG413862	[S8]
ndl-2	Scimone 2016	27063937	KT983961	[S9]
nlg7	Molina 2009	19174194	FJ471489	[S10]
nlg8	Molina 2009	19174194	FJ471490	[S10]
notum	Petersen 2011	21566195	JF725701	[S11]
opsin	Sanchez Alvarado 1999	10220416	AF112361	[S12]
PC2	Collins 2010	20967238	BK007043	[S13]
rootletin	Glazer 2010	19852954	AY068190	[S14]
sFRP-1	Petersen 2008	18063755	EU296635	[S15]
slit	Cebria 2007	17553481	DQ336176	[S16]
smad1	Molina 2007	17905225	EF633692	[S1]
smedwi-1	Reddien 2005	16311336	DQ186985	[S17]
wnt2	Petersen 2008	18063755	EU296634	[S15]
wnt5	Adell 2009	19211673	FJ463749	[S18]
zic-1	Vogg 2014	24704339	KF751216	[S4]

Supplemental Experimental Procedures

Animals and radiation treatment

Asexual *Schmidtea mediterranea* strain (CIW4) were maintained in 1x Montjuic planarian water at 20°C as previously described [S19]. Animals were starved 7–14 days prior experiments were used. Irradiated animals were exposed to a 6,000 rads dose of radiation using a dual Gammacell-40 ^{137}cesium source and amputated two days after irradiation. Animals were selected to be size-matched within an experiment, for all experiments.

Double-stranded RNA synthesis for RNAi experiments

Double stranded RNA (dsRNA) was synthesized as previously described [S20]. Briefly, PCR templates of sequences for the forward and reverse of the target genes were prepared with a 5' flanking T7 promoter (TAATACGACTCACTATAGGG). The forward and reverse templates (16 μl) were mixed, in separate reactions, with 1.6 μl of 100 mM rNTPs (Promega); 0.6 μl of 1M dithiothreitol (DTT; Promega); 4 μl of T7 polymerase; and 24 μl of 5x Transcription optimized buffer (Promega). Reactions were incubated for 2 h at 37°C and then supplemented with RNase-free DNase for 45 minutes. RNA was purified by ethanol precipitation, and finally resuspended in 24 μl of milliQ H2O. RNA was analyzed on 1% agarose gel. RNA for forward and reverse strands were combined and annealed by heating the reactions in a thermo-cycler to 90°C and lowering gradually the temperature to 20°C.

RNAi

Animals were starved for at least 7 days prior to the first feeding. The food mixture was as follows: 26 μl of 100% homogenized beef liver, 12 μl of dsRNA, and 2 μl of red food coloring. Animals were fed twice a week.

Transplantation and Microsurgery

Transverse trunk fragments were generated by amputation beneath the auricles and immediately posterior to the pharynx. Oblique fragments were generated by a single diagonal cut made from the right side of the animal adjacent to the right eye to the left side of the animal below the pharynx. Sagittal fragments were made by amputating the head and performing a single sagittal cut. Transplantation of pole and flank pieces was as follows. Large (10-12 mm long) animals were selected for the procedure. Donors were lethally irradiated (6000 rads) 24 hours prior to transplantation and then were incubated in a 1:500 dilution of DiI (2 μg/mL) in planarian water overnight (Figure S1A). Thirty minutes prior to transplantation the DiI solution was removed and the donors were transferred to fresh plates. Hosts were anesthetized in 0.2% chloretone diluted in planarian water for 5 minutes, and briefly rinsed in Holtfreter's before being place on a filter paper on ice moistened with Holtfreter's. Host heads were amputated to prevent the hosts from moving following the transplantation procedure, as has been previously described [S21]. A glass capillary tube of 0.75 mm interior diameter and 0.7 mm exterior diameter (FHC, Bowdoin, ME, USA) were used to remove host tissue from the future transplantation site posterior to the pharynx (Figure S1D) [S22]. Donors were placed on a filter paper on top of a petri-dish lid over ice moistened with Holtfreter's and either a pole fragment or flank fragment was excised (Figure S1B). Because donors were labeled with DiI, the donor fragments were easily visualized under a fluorescent microscope (Figure S1C). The pole or flank fragment was moved with a pipette from the donor to the host, and a pair of surgical scalpels were used to force the pole or flank fragment into the host (Figure S1E). The host was then placed in a recovery chamber as described previously [S22]. Twenty-four hours after transplantation, hosts were moved from the recovery chamber into a petri dish with planaria water. Live animals were examined under a fluorescent microscope to look for DiI signal (Figure S1G).

Fixations

Animals were fixed and labeled as previously described [S23]. In brief, animals were killed in 5% N-acetyl-cysteine in PBS for 5 minutes and then fixed in 4% formaldehyde for 20 minutes at room temperature. Fixative was removed and worms were rinsed 1X with PBSTx (PBS + 0.3% Triton X-100). PBSTx was replaced with preheated Reduction solution for 10 minutes at 37°C. Animals were dehydrated by a methanol series and stored in methanol at -20°C.

Whole-mount *in situ* hybridizations

RNA probes were synthesized and nitroblue tetrazolium/5-bromo-4-chloro-3-indolyl phosphate (NBT/BCIP) colorimetric whole-mount in situ hybridizations (ISH) were performed as described [S24]. Fluorescence in situ hybridizations (FISH) were performed as described [S23] with minor modifications. Briefly, animals were killed in

5% NAC and treated with proteinase K (4 μg/ml). Following overnight hybridizations, samples were washed twice in pre-hyb buffer, 1:1 pre-hyb-2X SSC, 2X SSC, 0.2X SSC, PBSTx. Subsequently, blocking was performed in 0.5% Roche Western Blocking Reagent (10% solution, Roche) and 5% inactivated horse serum PBSTx solution when anti-DIG or anti-DNP antibodies were used, and in 1% Roche Western Blocking Reagent PBSTx solution when an anti-FITC antibody was used. Post-antibody binding washes and tyramide development were performed as described [S23]. Peroxidase inactivation with 1% sodium azide was done for 90 minutes at RT. Most specimens were counterstained with DAPI overnight (Sigma, 1 μg/ml in PBSTx).

BrdU labeling and immunofluorescence

BrdU (Sigma) was administered by soaking fragments starting 1 hour following amputation for 2 hours in planaria H2O containing 25 mg/ml BrdU and 3% DMSO; animals were then chased in Instant Ocean dissolved at 5 g/L until they were fixed. For BrdU labeling, samples were pretreated by incubation in 2N HCl (+0.5% triton-X-100) for 45 minutes followed by brief neutralization in 0.1M sodium borate. BrdU was detected with mouse anti-BrdU (BD Biosciences) followed by goat anti-Mouse IgG HRP Conjugate (Life Technologies), blocked in 0.6% BSA, 1% Western Blocking Reagent (Roche), and 5mM thymidine in PBSTx(0.3%). The BrdU signal was developed as previously described [S24] using the Cy5 tyramide.

***en face* mounting**

Following staining, animals were placed in a petri dish with PBSTx and the anterior blastemas were cut off using a sharp scalpel. The anterior blastemas were placed on a slide with the cut edge down. A coverslip was placed over the same and Vectashield was allowed to flow in from the side.

Microscopy and image analysis

Fluorescent images were taken with a Zeiss LSM700 Confocal Microscope. Light images were taken with a Zeiss Discovery Microscope. For *en face* images, the marking of cell positions was performed using Fiji/ImageJ. A text file containing the positions of all the cells, and 5 reference positions (Figure S2A), was exported from Fiji/ImageJ. Reference point 1 is the dorsal most point, reference point 2 is the ventral most point, reference points 3 and 4 are the right and left sides, respectively, and reference point 5 is the estimated DV boundary in the blastema. This file was imported into MATLAB, which was used to perform the following transformations:

Coordinate Transformation I: The mean of reference points 1 and 2 was subtracted from all coordinates. This moves the distribution so that rotation will be around this point.

Coordinate Rotation: Matrix multiplication was used to rotate the coordinates so that reference point 1 was directly vertical.

Coordinate Transformation II: The x-value mean of reference points 3 and 4 was used to subtract from the X coordinates, and the y-value of reference point 5 was used to subtract from the Y coordinates. This places the origin of the data at the middle between the right and left sides of the fragment, and at the DV boundary.

The transformed coordinates, as well as measurements of distances between the coordinates and various landmarks were exported into an Excel document for further analysis. The histogram function in Excel was used on the X coordinates to generate the histograms for Figures 1D, 2B, 3C-D, S2C, S2F. The Y coordinates were plotted to generate Figures 1E, 2C, 4C-E, 4G-H, S2D, and S2G. The absolute values of the Y coordinates were used to generate the distances from the DV boundary in Figures 1F, 2E, S2E, S2H, and S2I.

Graphs and statistical analysis

All graphs and statistical analysis were done using the Prism software package (GraphPad Inc., La Jolla, CA). Comparisons between the means of two populations were done by a Student's t-test. Comparisons between two distributions were done using a Mann-Whitney test. Comparisons between two rows in a contingency table were done using Fisher's exact test. Significance was defined as $p < 0.05$.

Supplemental References

S1. Molina, M.D., Saló, E., and Cebrià, F. (2007). The BMP pathway is essential for re-specification and maintenance of the dorsoventral axis in regenerating and intact planarians. Dev. Biol. *311*, 79–94.

S2. Oviedo, N.J., Newmark, P.A., and Sánchez Alvarado, A. (2003). Allometric scaling and proportion regulation in the freshwater planarian *Schmidtea mediterranea*. Dev. Dyn. *226*, 326–33.

S3. Roberts-Galbraith, R.H., and Newmark, P.A. (2013). Follistatin antagonizes Activin signaling and acts with Notum to direct planarian head regeneration. Proc. Natl. Acad. Sci. U. S. A. *110*, 1363–8.

S4. Vogg, M.C., Owlarn, S., Pérez Rico, Y.A., Xie, J., Suzuki, Y., Gentile, L., Wu, W., and Bartscherer, K. (2014). Stem cell-dependent formation of a functional anterior regeneration pole in planarians requires Zic and Forkhead transcription factors. Dev. Biol. *390*, 136–48.

S5. Nishimura, K., Kitamura, Y., Umesono, Y., Takeuchi, K., Takata, K., Taniguchi, T., and Agata, K. (2008). Identification of glutamic acid decarboxylase gene and distribution of GABAergic nervous system in the planarian *Dugesia japonica*. Neuroscience. *153*, 1103–14.

S6. Tazaki, A., Kato, K., Orii, H., Agata, K., and Watanabe, K. (2002). The body margin of the planarian *Dugesia japonica*: characterization by the expression of an intermediate filament gene. Dev. Genes Evol. *212*, 365–73.

S7. Zayas, R.M., Cebrià, F., Guo, T., Feng, J., and Newmark, P.A. (2010). The use of lectins as markers for differentiated secretory cells in planarians. Dev. Dyn. *239*, 2888–97.

S8. Wenemoser, D., and Reddien, P.W. (2010). Planarian regeneration involves distinct stem cell responses to wounds and tissue absence. Dev. Biol. *344*, 979–91.

S9. Scimone, M.L., Cote, L.E., Rogers, T., and Reddien, P.W. (2016). Two FGFRL-Wnt circuits organize the planarian anteroposterior axis. eLife. *5*, e12845.

S10. Molina, M.D., Saló, E., and Cebrià, F. (2009). Expression pattern of the expanded noggin gene family in the planarian *Schmidtea mediterranea*. Gene Expr. Patterns. *9*, 246–53.

S11. Petersen, C.P., and Reddien, P.W. (2011). Polarized *notum* activation at wounds inhibits Wnt function to promote planarian head regeneration. Science. *332*, 852–5.

S12. Sánchez Alvarado, A., and Newmark, P.A. (1999). Double-stranded RNA specifically disrupts gene expression during planarian regeneration. Proc. Natl. Acad. Sci. U. S. A. *96*, 5049–54.

S13. Collins, J.J., Hou, X., Romanova, E. V., Lambrus, B.G., Miller, C.M., Saberi, A., Sweedler, J. V, and Newmark, P.A. (2010). Genome-wide analyses reveal a role for peptide hormones in planarian germline development. PLoS Biol. *8*, e1000509.

S14. Glazer, A.M., Wilkinson, A.W., Backer, C.B., Lapan, S.W., Gutzman, J.H., Cheeseman, I.M., and Reddien, P.W. (2010). The Zn finger protein Iguana impacts Hedgehog signaling by promoting ciliogenesis. Dev. Biol. *337*, 148–56.

S15. Petersen, C.P., and Reddien, P.W. (2008). *Smed-betacatenin-1* is required for anteroposterior blastema polarity in planarian regeneration. Science. *319*, 327–30.

S16. Cebrià, F., Guo, T., Jopek, J., and Newmark, P.A. (2007). Regeneration and maintenance of the planarian midline is regulated by a *slit* orthologue. Dev. Biol. *307*, 394–406.

S17. Reddien, P.W., Oviedo, N.J., Jennings, J.R., Jenkin, J.C., and Sánchez Alvarado, A. (2005). SMEDWI-2 is a PIWI-like protein that regulates planarian stem cells. Science. *310*, 1327–30.

S18. Adell, T., Salò, E., Boutros, M., and Bartscherer, K. (2009). Smed-Evi/Wntless is required for β-catenin-dependent and -independent processes during planarian regeneration. Development. *136*, 905–10.

S19. Sánchez Alvarado, A., Newmark, P.A., Robb, S.M.C., and Juste, R. (2002). The *Schmidtea mediterranea* database as a molecular resource for studying platyhelminthes, stem cells and regeneration. Development. *129*, 5659–65.

S20. Rouhana, L., Weiss, J.A., Forsthoefel, D.J., Lee, H., King, R.S., Inoue, T., Shibata, N., Agata, K., and Newmark, P.A. (2013). RNA interference by feeding in vitro synthesized double-stranded RNA to planarians: methodology and dynamics. Dev. Dyn. *242*, 1–43.

S21. Santos, F. V. (1929). Studies on transplantation in planaria. Biol. Bull. *57*, 188–97.

S22. Guedelhoefer, O.C., and Sánchez Alvarado, A. (2012). Amputation induces stem cell mobilization to sites of injury during planarian regeneration. Development. *139*, 3510–20.

S23. King, R.S., and Newmark, P.A. (2013). In situ hybridization protocol for enhanced detection of gene expression in the planarian *Schmidtea mediterranea*. BMC Dev. Biol. *13*, 8.

S24. Pearson, B.J., Eisenhoffer, G.T., Gurley, K.A., Rink, J.C., Miller, D.E., and Sánchez Alvarado, A. (2009). A Formaldehyde-based Whole-Mount In Situ Hybridization Method for Planarians. Dev. Dyn. *238*, 443–50.